



iJRASET

International Journal For Research in
Applied Science and Engineering Technology



INTERNATIONAL JOURNAL FOR RESEARCH

IN APPLIED SCIENCE & ENGINEERING TECHNOLOGY

Volume: 5 Issue: VI Month of publication: June 2017

DOI:

www.ijraset.com

Call:  08813907089

E-mail ID: ijraset@gmail.com

A Copper Based Metal Organic Framework: Dynamic Green Catalyst for Heterogeneous O- Acetylation of Alcohols Under Solvent Free Condition.

S. Santhana Laxmi¹, V. Murugesan², K. Usha Nandhini³

^{1,3}Department of Chemistry, Queen Mary's College (A), Chennai- 600 004, Tamilnadu, India.

²Department of Chemistry, B.S. Abdur Rahman University, Chennai- 600 045, Tamilnadu, India.

Abstract: The metal-organic framework material $Cu_3(BTC)_2$ was synthesized solvothermally using copper nitrate trihydrate as metal source, benzene 1,3,5 tricarboxylic acid as ligand, dimethyl formamide, ethanol and deionized water as solvents. The new layered hybrid material thus obtained was characterized by several techniques such as powder X-ray diffraction spectroscopy (P-XRD); electron spin resonance spectroscopy (ESR) and fourier transform-infra red spectroscopy (FT-IR). The porosity of the synthesized material was characterized by BET analysis. The textural properties were analysed by scanning electron microscopy (SEM). The stability of the synthesized material was analysed by thermo gravimetric analyser (TGA). The catalytic performance of the $Cu_3(BTC)_2$ MOF was explored for O-acetylation of alcohols under solvent free condition at 353 K. The catalytic activity of the synthesized MOF was followed using gas chromatography (GC).

Keywords - Metal-organic frameworks, $Cu_3(BTC)_2$, Solvothermal synthesis, Heterogeneous catalysis, O-acetylation.

I. INTRODUCTION

Metal-organic frameworks (MOFs, also known as porous coordination polymers or PCPs) are crystalline hybrid materials constructed from metal ions or clusters bridged by organic linkers to form one-, two-, or three dimensional networks [1]. Bivalent or trivalent aromatic carboxylic acids and N-containing aromatic ligands are commonly used to form frameworks with zinc, copper, chromium, aluminium, magnesium and other elements [2-6]. As organic components, rigid molecules (such as conjugated aromatic systems) are usually preferred over flexible ones [7, 8], since they favor the formation of crystalline, porous, stable MOFs. Generally the synthetic method consists of mixing two solutions containing the metal and the organic component, either at room temperature or under (hydro) solvothermal conditions and with or without the use of additional auxiliary molecules. The nature of the solvent, the ligands, or the presence of cations and other guest molecules in the synthesis of MOFs can have a dramatic effect on the crystal structure of the material obtained. Thus, a given metal-ligand combination can lead to a number of different structures (polymorphism), depending on subtle changes on the above-mentioned synthesis parameters.

MOFs are becoming one of the most rapidly developing fields in chemistry, chemical engineering and material sciences and emerging as an important family of porous materials not only because of their intriguing network topologies but also due to their large surface areas, tunable pore sizes and versatile architectures. These outstanding features make MOFs promising materials for use in applications such as gas adsorption and separation [9, 10], heterogeneous catalysis [11-16], sensing [17], luminescence [18], proton conduction [19], and drug delivery [20]. In particular, MOFs have attracted much attention in organic catalysis [12], asymmetric catalysis [15] and photocatalysis [13]. Heterogeneous catalysis is playing an increasingly imperative role in chemical manufacturing, often with the result of a major reduction in waste [21]. For economic and environmental reasons, there is a huge incentive to replace homogeneous by green and efficient heterogeneous catalytic systems. Heterogeneous catalysis is superior to homogeneous because of easier separation, reusability, minimized waste, green and clean products [22]. Moreover, the high metal content in MOFs, high surface area and crystalline structure, their insolubility in water and common organic solvents and as well as their potential ability as shape-, size-, chemo-, and enantio- selective catalysts, offers immense scope for their exploration as heterogeneous catalyst [23]. The use of MOFs as heterogeneous catalysts has presented a significant increase in the last two decades as they have been considered as eco-friendly alternatives for catalysis. Separation of the reaction products and the catalyst reusability, less leaching problems make MOFs as active heterogeneous catalysts.

International Journal for Research in Applied Science & Engineering Technology (IJRASET)

Most of the work has been focused on the synthesis and characterization of MOFs. So far, only few catalytic applications of metal organic frameworks have been reported. Therefore we have screened a number of known MOFs and selected a well known hybrid material in which metal coordination sites are accessible from the pore interior for the heterogenous catalysis reaction. A compound fulfilling these requirements is $\text{Cu}_3(\text{BTC})_2$. Crystal structure of $\text{Cu}_3(\text{BTC})_2$, was first reported in 1999 by Chui et al [24]. It is one of the best characterized and widely studied MOF materials thus far, and it is also known as HKSUT-1. Recently Wang et al have studied the potential use of $\text{Cu}_3(\text{BTC})_2$ for gas purification and separation [25].

Our interest is to explore the catalytic properties of $\text{Cu}_3(\text{BTC})_2$ MOF material for o-acetylation of alcohols, being a fundamental step in many organic syntheses. Hydroxyl groups are present in a number of compounds in biological and synthetic interest. Among the protecting groups for alcohols, esters are the most important with acetate being the easiest of all. A number of copper salts have been used in homogeneous catalyst for O- acetylation of alcohols [26-28], but they suffer from drawbacks of difficulty in catalyst and product separation, and result in permanent deactivation of the catalyst which directly adds the catalyst to the waste stream [29]. Hence introduction of new methods, greener and better catalyst with easily recycled and reusability for the preparation of esters is still in demand. In light of this interest, we report the heterogeneous catalytic activity of $\text{Cu}_3(\text{BTC})_2$ MOF material for O-acetylation of alcohols under solvent free condition.

II. EXPERIMENTAL

A. Materials

Copper (II) nitrate trihydrate [$\text{Cu}(\text{NO}_3)_2 \cdot 3\text{H}_2\text{O}$, Sigma Aldrich, 99%], Benzene 1,3,5 tricarboxylic acid [BTC, Sigma Aldrich, $\text{C}_9\text{H}_6\text{O}_6$, 95%]. The solvents, ethyl alcohol anhydrous [$\text{C}_2\text{H}_5\text{OH}$, Merck 99.9%], N,N-dimethylformamide [DMF, $\text{HCON}(\text{CH}_3)_2$, Merck 99.5%], deionized (DI) water were used in the catalyst synthesis. All the chemicals used for O-acetylation conversion were of analytical grade and used without further purification.

B. Catalyst Preparation

$\text{Cu}(\text{NO}_3)_2 \cdot 3\text{H}_2\text{O}$ (1.75 g) and BTC (0.84 g) were added in 125 ml solvent mixture containing water, ethanol and DMF in the ratio 1:1:1. This mixture was stirred for two hours on a magnetic stirrer. Then the resulting mixture was transferred into a 250 ml teflon lined stainless steel autoclave and allowed to react at 393 K without stirring. After 18 h the autoclave was allowed to cool. A light blue colored material was collected by filtration and washed with water. After the solid product had been obtained, solvent exchange was carried out with dichloromethane (DCM) (3×10 ml) at room temperature for 3 days. The product was then filtered and dried under vacuum at 373 K for 6 h. A crucial point in preparing porous MOF-based materials is the solvent exchange, as this step will facilitate the evacuation of the material frameworks. The occluded DMF in the as-synthesized MOF sample were exchanged with DCM by immersion, replacing the strongly interacting guest formamide solvent molecules with more weakly interacting DCM molecules that would be easily removed under vacuum. This step would minimize the problems of pore blockage and framework collapse in the ordered structure [30].

C. Physicochemical Characterization

The porous metal organic framework was characterized by powder X-ray diffraction (p-XRD), electron spin resonance spectroscopy (ESR), BET surface area, pore size, pore volume, fourier transform infrared spectroscopy (FT-IR), thermogravimetric analysis (TGA), energy dispersive X-ray spectroscopy (EDXS), scanning electron microscopy (SEM). The products of the catalytic reaction was separated using Gas chromatography (GC) and were confirmed using Gas Chromatography – Mass spectrometry (GC-MS).

The crystalline structure of material was investigated on a Bruker D8 advance powder X-ray diffraction system with operating voltage 40 KV per 30 mA current rating with Cu – K α radiation ($\lambda = 0.154$ nm). The diffractograms were recorded in the 2θ range $10-70^\circ$ with a 2θ step size of 0.02° and a count time of 10s at each point. EPR studies were done to understand the oxidation state of the metal sites in the material. The sample was transferred into EPR quartz tube and evacuated for 48 h at 107 K and sealed. EPR data was recorded with an X-band at 300 K with frequency 9445.460 MHz, power 0.99800 mW, field center 400.000 mT, width 400.000 mT, sweep time 4.0 min from JES-FA 200 instrument. Textural properties of the catalysts were studied using a Quanta Chrome NOVA 1000 surface analyzer by nitrogen adsorption at 77 K. Prior to measurement, samples were degassed to remove preadsorbed gas and moisture at 573 K for 4 h. This instrument employed the BET method by measuring the quantity of nitrogen absorbed, and the cumulative volume and diameter of pores were obtained by the BJH method from the desorption isotherms [31]. FT-IR spectra of the material was recorded on Perkin Elmer spectrum one FT-IR spectrometer using KBr pellets. The pellet was used to record the infrared spectra in the range $450 - 4000$ cm^{-1} with the typical resolution of 1.0 cm^{-1} . Thermogravimetric analysis

International Journal for Research in Applied Science & Engineering Technology (IJRASET)

was performed on TGA (Perkin Elmer) Q500 Hi-Res TGA from thermal analyser instrument, in order to find the stability of the synthesized material. The morphology of the synthesised MOF material was examined by scanning electron microscopy (SEM). The SEM analysis was done using Supra Zeiss instrument with resolution of 1mm at 30 KV with 20 mm Oxford EDS detector. Before measurement, the MOF sample suspended in ethanol was dropped onto a silicon plate and dried at room temperature.

D. Catalytic Studies

O-acetylation of alcohols with acetyl chloride was carried out in liquid phase. Alcohol (2 mmol), acetyl chloride (4 mmol) and $\text{Cu}_3(\text{BTC})_2$ (20% w.r.t. alcohol) were taken in a 25 ml round bottomed flask fitted with a reflux condenser. The flask with its contents was heated at a constant temperature in an oil bath and stirred magnetically. Aliquots of the hot mixture were withdrawn at regular intervals to monitor the progress of the reaction [32]. The reaction mixture was diluted with diethyl ether (10 ml) and centrifuged. The supernatant liquid was decanted and diethyl ether (5 ml) was again added to the solid mass and centrifuged. The decanted aliquots were combined and washed with 10 % sodium bicarbonate solution and then with water. The organic layer was separated and dried and then concentrated to get the crude product, which was then dissolved in ethanol. The liquid products thus obtained were characterized using gas chromatography (GC). The clarus 680 GC was used in the analysis employed with a fused silica column, packed with elite-5 MS (5% biphenyl, 95% dimethyl polysiloxane, 30 m x 0.25 mm x 250 μm) and the components were separated using helium as carrier gas at a constant flow of 1 ml/min. The products were identified using GC-MS (Perkin-Elmer instrument). The clarus 600 (EI) turbo mass spectrometer (EI 70eV) was used to detect the mass of the product. The spectrum of the components were compared with the database of spectrum of known components stored in the GC-MS (NIST-2008) library.

III. RESULTS AND DISCUSSION

A. Characterization of the Catalyst.

X-Ray diffraction is an effective method to investigate the crystalline properties of the synthesized material. The XRD pattern for $\text{Cu}_3(\text{BTC})_2$ is shown in the Fig-1. High intensity Bragg diffraction peaks are observed at $2\theta = 12.17^\circ, 13.6^\circ, 18.99^\circ, 29.31^\circ, 35.14^\circ, 39.04^\circ$ & 41.47° and with few low intensity peaks. The peak of highest intensity at $2\theta = 12.17^\circ$ is indexed as d_{100} for copper. The average crystallite size (D) from x-ray line broadening was calculated using the Scherrer equation (1) [33],

$$D = \frac{0.9\lambda}{\beta_{1/2} \cos\theta} \quad (1)$$

where λ is the wavelength of the X-ray, $\beta_{1/2}$ is the angular width at the half maximum intensity and θ is the Bragg's angle. The XRD patterns of the Cu-BTC obtained was found to coincide closely with the $\text{Cu}_3(\text{BTC})_2$ reported in literature [24, 34]. The crystallographic data of the synthesised material are confirmed by EXPO 2014 software and are presented in Table 1.

ESR spectrum of the synthesized metal organic framework is shown in Fig. 2. X band continuous wave (cw) ESR measurement of the synthesized material at 303 K shows a broad line with a g value 2.14. We assign this signal to the antiferromagnetically coupled Cu^{2+} dimers with $S = 1$ of the binuclear carboxylates building units of the $\text{Cu}_3(\text{BTC})_2$ framework [35]. Also we have to note that the ESR spectra in Figure 2 do not show the typical features of an $S = 1$ spin system as observed for a number of different dimeric Cu^{2+} species [36] but only a broad line is detected with a g value corresponding to the average g value of these Cu^{2+} dimers. Therefore, we assume that spin exchange between the interconnected copper dimers is taking place across the BTC ligands in the $\text{Cu}_3(\text{BTC})_2$ framework leading to an averaging of the anisotropic spectral features of the individual $S=1$ Cu^{2+} dimer spectra [35, 37].

The textural properties of the $\text{Cu}_3(\text{BTC})_2$ MOF material before and after solvent exchanged are presented in Table 2. Surface area of the material was found to be $700 \text{ m}^2/\text{g}$ [38, 39]. The presence of copper in the framework has a significant effect on the specific surface area A_{BET} and pore volume V_p and pore diameter d_p . The activation step, which is the removal of unreacted metal salts, organic ligands, or solvents from the MOF interior, is a key factor in producing high surface area MOFs. In particular, $\text{Cu}_3(\text{BTC})_2$ solvent exchanged via dichloromethane exhibited significantly improved textural properties.

Fourier transforms infrared spectroscopy (FT-IR) of copper MOF confirms the formation of $\text{Cu}_3(\text{BTC})_2$ (Fig-3). The broad band at 3336 cm^{-1} is due to aromatic C-H stretching vibration originating from trimesic acid (Benzene 1,3,5 tricarboxylic acid). The bands at 1617 and 1542 cm^{-1} respectively are due to C-O asymmetric stretching vibration originating from the carbonyl C-O of the carboxylic acid and C-C skeletal vibration of the benzene ring. The weak band at 1446 cm^{-1} is due to C-O symmetric stretching vibration from the carboxyl group of the trimesic acid. The strong band at 1365 cm^{-1} is due to C-O stretching vibration. The absorption bands at $937-1112 \text{ cm}^{-1}$ can be assigned to the O-C-O symmetric and asymmetric stretching vibrations. The strong bands

International Journal for Research in Applied Science & Engineering Technology (IJRASET)

at 720-760 cm^{-1} are probably due to Cu(II)-O vibrations in agreement with the literature reports [40, 41].

The thermal stability of the synthesised material was confirmed by TGA. The Fig. 4 shows two step weight loss while increasing the temperature; initial weight change (6% - 12%) occurs near 356 K due to dehydration of the $\text{Cu}_3(\text{BTC})_2$ material. A second weight loss (35%) found around 600 K may be due to decomposition of the organic framework [42]. Thus the $\text{Cu}_3(\text{BTC})_2$ material was stable upto 600 K. The TGA curve of the material is shown in Fig. 4. The chemical composition of the synthesised material was studied by means of energy dispersive X-ray spectroscopy (EDXS). The EDXS pattern of $\text{Cu}_3(\text{BTC})_2$ MOF is shown in Fig. 5 [33]. The EDXS pattern confirms the presence of copper, carbon and oxygen. Quantitative analysis of the EDXS result is summarized in Table 3.

Scanning electron micrograph of $\text{Cu}_3(\text{BTC})_2$ MOF at 10, 30 and 50 μm are shown in Fig. 6. Scanning electron microscopy is a technique that enables the study of the microstructure of nanoparticles of matter. The different magnification SEM images at 10, 30 and 50 μm of the synthesized material shows cubic octahedral morphology. The morphology of $\text{Cu}_3(\text{BTC})_2$ framework is closely in consistent with the previous reports [43, 44, 45].

B. Catalytic Studies

The catalytic activity of the synthesized MOF material for alcohol conversion was explored by using 20 wt % of MOF at different temperatures under solvent free condition. Various primary and secondary based aliphatic and aromatic alcohols involved in acetylation reaction with acetyl chloride provided high yield of the desired esters. Aromatic alcohols having electron donating group or electron withdrawing group reacted efficiently with acetyl chloride providing the esters in excellent yields. This protocol was also applicable for acetylation of long chain aliphatic alcohols providing the desired esters in good yields [29]. Following this, acetylation of various aliphatic and aromatic alcohols with acetyl chloride has been studied in the present work.

1) *Effect of Temperature*: In order to optimize the reaction condition, the effect of temperature on acetylation of alcohols was investigated. The reaction was carried out at 323, 353 and 373 K for 2 h. The GC analysis results were shown in Table 4. Notably the yield of the corresponding esters increased with an increase in temperature up to 353 K. Further increase in temperature to 373 K did not have much effect on the yield. Hence we optimized the reaction temperature to 353 K. It was found that though open chain aliphatic alcohols had 100% conversion to give expected esters (product I in Table 5.), the obtained product I underwent further reaction with acetyl chloride thus converting the initially formed ester to more stable product (product II) as presented in the Table 5. This may be due to free access of acetylating agent to the active sites. Table 5 represents the O-acetylation of alcohols catalysed by $\text{Cu}_3(\text{BTC})_2$ MOF at 353 K.

2) *Effect of Catalyst*: The O-acetylation reaction of alcohols was also carried out with and without the use of $\text{Cu}_3(\text{BTC})_2$ catalyst at 353 K. The GC results were shown in Fig. 7. $\text{Cu}_3(\text{BTC})_2$ catalyst exhibited excellent catalytic activity with wide range of substrates whereas in the absence of catalyst the reaction provided very low conversion with no significant yield. This is due to the free metallic sites in the $\text{Cu}_3(\text{BTC})_2$ framework, which interact with C-O group of the acetyl chloride thereby activating the acetyl group of the acetyl chloride and enhancing the leaving ability of the acetate counterpart. The activated acetyl chloride on the catalyst surface reacts with the alcohol to give ester as a product.

3) *Effect of Time*: O-acetylation of alcohol was carried out at the optimized temperature for different reaction times over $\text{Cu}_3(\text{BTC})_2$ catalyst. The time study of the reaction was monitored every 30 minutes using Gas Chromatograph. Fig. 8 represents the acetylation of benzyl alcohol for different time periods. Initially the alcohol conversion proceeds comparatively fast with increase in time and becomes slow at the later period. The probable reason may be that the esters competes with the reactant for similar surface sites of the catalyst thereby inhibiting its adsorption on the catalyst surface [32]. Thus an increase in the concentration of the product decreases the rate of the reaction as only few sites are left for the reactant to get activated. Similar the results are found for other substrates involved in the reaction.

4) *Effect of Feed Ratio*: The effect of feed ratio on alcohol conversion was examined over 20 wt% of MOF with 1:2, 1:4, 1:6 (alcohol:acetyl chloride) at 353 K for 2h.. The results are presented in Table 6. Conversion decreases with increase in the feed. Esters are observed at very high yield only with feed ratio 1:2 but not with other feeds. There is a sudden drop in the conversion for change of feed ratio from 1:2 to 1:6. The reason for the decrease may be due to inadequate number of active sites in the catalyst surface to chemisorb the acetylating agent at the higher feed ratios [32]. Table 6 represents the alcohol conversion of benzyl alcohol with different feed ratios. The results are found to be in consistent with other aliphatic and aromatic alcohols.

5) *Reusability of the Catalyst*: To evaluate the stability of the $\text{Cu}_3(\text{BTC})_2$ catalyst in the liquid phase reaction, a catalyst recycling test was performed at 353 K. The used catalyst samples recovered from the reaction mixture by filtration was washed with

International Journal for Research in Applied Science & Engineering Technology (IJRASET)

diethylether and dried in air for 24 h. The catalyst was activated at 373 K in air for 2 h prior to the next run and was reused up to three times in reaction with fresh reagents. The result of the benzyl alcohol conversion is shown in Fig. 9. Similar results are found for other substrates. $\text{Cu}_3(\text{BTC})_2$ catalyst shows considerable reduction in catalytic activity as noticed by the amount of esters obtained. However, no abrupt change was observed, which confirms that $\text{Cu}_3(\text{BTC})_2$ is a stable and efficient heterogeneous catalyst for O-acetylation of alcohols.

IV. CONCLUSIONS

In summary, we have demonstrated that the synthesized $\text{Cu}_3(\text{BTC})_2$ MOF is an highly efficient heterogeneous catalyst for the O-acetylation reaction towards various aromatic and aliphatic alcohols. The catalytic reaction displays remarkable yields with high selectivity in a short reaction time under heterogeneous conditions. Notably, the catalyst can be recycled and reused several times without any major loss of activity. Moreover, no organic solvent is necessary for the reaction, which makes the catalysis really green. Further investigation of the application of copper based framework catalysts towards various organic conversions are currently in progress in our laboratory.

V. ACKNOWLEDGMENT

The authors thank profusely Science and Engineering Research Board (SERB), New Delhi, for the sanction of funds under Start-Up Research Grant (Young Scientists) – Chemical Sciences No.SB/FT/CS-061/2012.

REFERENCES

- [1] z.j. Lin, m. Hong, r. Cao, *chem. Soc. Rev.*, 43, 5867-5895 (2014).
- [2] y.r. Lee, j. Kim, w.s. Ahn, *korean j. Chem.eng.*, 30, 1667 (2013).
- [3] d. J. Tranchemontagne, j. L. Mendoza-cortes, m. O'keeffe and o.m. Yaghi, *chem. Soc. Rev.*, 38, 1257 (2009).
- [4] a. U. Czaja, n. Trukhan and u. Müller, *chem. Soc. Rev.*, 38, 1284 (2009).
- [5] d. Zhao, d.q. Yuan, d. F. Sun and h. C. Zhou, *j. Am. Chem. Soc.*, 131, 9186 (2009).
- [6] d. Yuan, d. Zhao, d. Sun and h. C. Zhou, *angew. Chem., int. Ed.*, 49, 5357 (2010).
- [7] a. Corma, h.garcia, and f.x. Llabres i xamena, *chem. Rev.*, 110, 4606-4655 (2010).
- [8] s. M.hawxwell, g. M. Espallargas, d. Bradshaw, m. J. Rosseinsky,t. J. Prior, a.j. Florence, j.van de streek,l. Brammer, *chem. Commun.*, 1532 (2007).
- [9] y.b. Huang, j.liang, x.s. Wang and r.cao, *chem. Soc. Rev.*, 46, 126-157 (2017).
- [10] k. Sumida, d. L. Rogow, j. A. Mason, t. M. Mcdonald, e. D. Bloch, z. R. Herm, t.-h. Baeand j. R. Long, *chem. Rev.*, 112, 724–781 (2012).
- [11] j. Liu, l. Chen, h. Cui, j. Zhang, l. Zhang and c.-y. Su, *chem. Soc. Rev.*, 43, 6011–6061 (2014).
- [12] a. Dhakshinamoorthy, a. M. Asiri and h. Garcia, *chem. Soc. Rev.*, 44, 1922–1947 (2015).
- [13] t. Zhang and w. Lin, *chem. Soc. Rev.*, 43, 5982–5993 (2014).
- [14] a. H. Chughtai, n. Ahmad, h. A. Younus, a. Laypkovc and f. Verpoort, *chem. Soc. Rev.*, 44, 6804–6849 (2015).
- [15] y. Liu, w. Xuan and y. Cui, *adv. Mater.*, 22, 4112–4135 (2010).
- [16] l. Ma, c. Abney and w. Lin, *chem. Soc. Rev.*, 38, 1248–1256 (2009).
- [17] z. Hu, b. J. Deibert and j. Li, *chem. Soc. Rev.*, 43, 5815–5840 (2014).
- [18] y. Cui, y. Yue, g. Qian and b. Chen, *chem. Rev.*, 112, 1126–1162 (2012).
- [19] k. Fujie and h. Kitagawa, *coord. Chem. Rev.*, 307, 382–390 (2016).
- [20] m. Gime'nez-marque's, t. Hidalgo, c. Serre and p. Horcajada, *coord. Chem. Rev.*, 307, 342–360 (2016).21. A.h. Chughtai, n.ahmad, h.a. Younus, a.laypkov and f.verpoort, *chem. Soc. Rev.*, 44, 6804–6849 (2015).
- [22] m. Fujita, y. J. Kwon, s. Washizu and k. Ogura, *j. Am. Chem. Soc.*, 116, 1151–1152 (1994).
- [23] p. Horcajada, c. Serre, g. Maurin, n. A. Ramsahye, f. Balas, m. Vallet-regi, m. Sebban, f. Tauler and g. Ferey, *j. Am. Chem. Soc.*, 130, 6774 (2008).
- [24] s.s.y. Chui, s.m.f. Lo, j.p.h. Charmant, a.g. Orpen, i.d.williams, *science.*, 283, 1148 (1999).
- [25] q.m. Wang, d.m. Shen, m. Bülw, m.l. Lau, s.g. Deng, f.r. Fitch, n.o. Lemcoff, j. Semanscin, *micropor. Mesopor. Mater.*, 55, 217(2002).
- [26] k. Jeyakumar, d.k. Chand, *j. Mol. Catal. A. Chem.*, 255, 275 (2006).
- [27] k.l. Chandra, p. Saravanan, r.k. Singh, v.k. Singh, *tetrahedron.*, 58, 1369 (2002).
- [28] r.k. Khunger, *synlett.*, 327 (2006).
- [29] s.j. Singh, s.r. Kale, m.b. Gawande, a.velhinho, r.v. Jayaram, *cat. Comm.*, 44, 24-28 (2014).
- [30] n.t.s. Phan, k.k.a. Le, t.d. Phan, *appl. Catal. A: gen.*, 218, 25–30(2001).
- [31] s.ramesh and n.j. Venkatesha, *acs sustainable chem. Eng.*, 5, 1339-1346 (2017).
- [32] k.ushanandhini, b. Arabindoo, m. Palanichamy, v. Murugesan., *micropor. Mesopor. Mater.*, 81, 59-71 (2005).
- [33] e.d. Dikio and a.m. Farah, *chemsci trans.*, 2(4), 1386-1394 (2013).
- [34] k. Schlichte, t. Kratzke and s. Kaskel, *micropor. Mesopor. Mater.*, 73, 81 (2004).
- [35] w.bohlmann, a.poopl, m.sabo and s. Kaskel, *j. Phys. Chem. B.*, 110, 20177-20181 (2006).
- [36] a. Bencini, d.gatteschi, *epi of exchanged coupled systems.*, springer: berlin (1990).
- [37] a. Poppl, s.kunz, d.himsl and m. Hartmann, *j. Phys. Chem. B.*, 112, 2678-2684 (2008).
- [38] j.kim, h.y. Cho, w.s. Ahn, *catal surv asia.*, 16, 106-119 (2012).
- [39] s.t. Meek, j.a. Greathouse, m.d. Allendorf, *chemcommun.*, 47, 11650 (2011).
- [40] g. Cordoba, r. Arroyo, j.l.g. Fierro, m. Viniestra, *j. Solid state chem.*, 123, 93 (1996).

International Journal for Research in Applied Science & Engineering Technology (IJRASET)

- [41] e.m. Fixman, m.c. Abello, o.f. Goriz, I.a. Arrua, appl. Catal. A., 319, 111 (2007).
- [42] j.l.c. Rowsell, a.r. Millward, k.s. Park, o.m. Yaghi, j. Am. Chem.soc., 126, 5666 (2004).
- [43] m. Klimakow, p. Klobes, a.f. Thunemann, k. Rademann, f. Emmerling, chem. Mater., 22, 5216 (2012).
- [44] m.m. Peng, h.t. Jang and m.palanichamy, int. J. Cont. Autom., 6 (6), 1-12 (2013).
- [45] z. H. Xiang, d. P. Cao, x. H. Shao, w. C. Wang, j. W. Zhang and w. Z. Wu, chemical engineering science., 65, 3140 (2010).

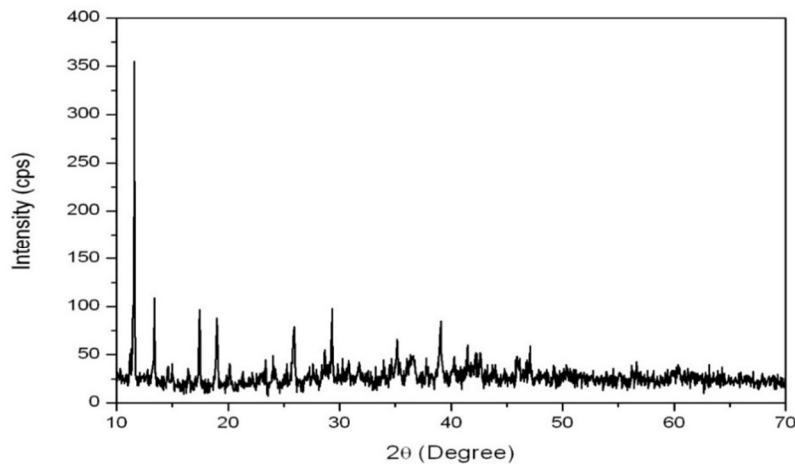


Fig.1 X-ray powder diffraction pattern of $\text{Cu}_3(\text{BTC})_2$ MOF.

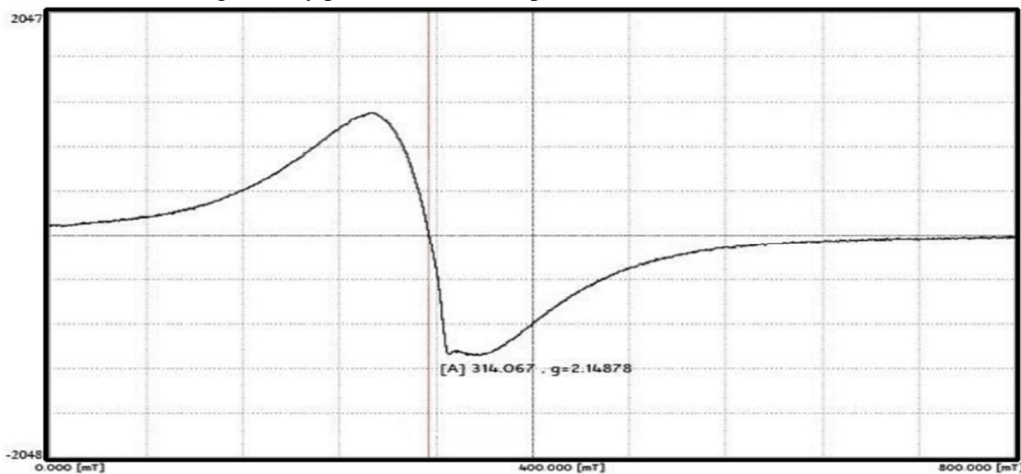


Fig. 2 ESR spectrum of $\text{Cu}_3(\text{BTC})_2$ MOF at 303 K.

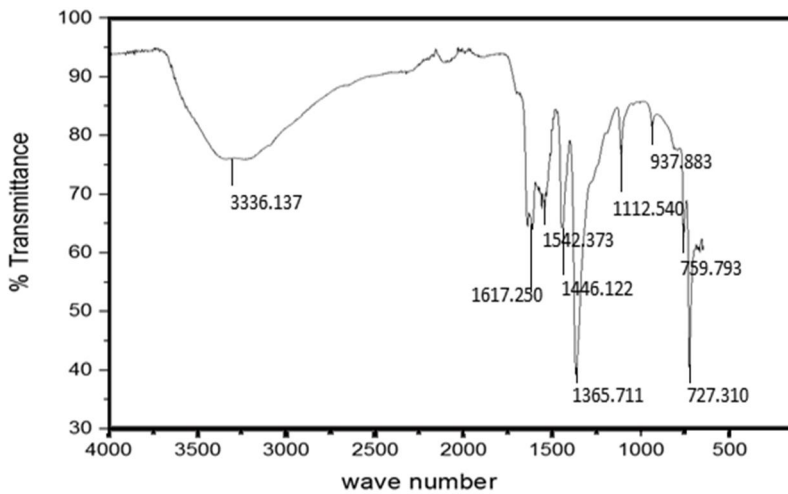


Fig. 3 FT-IR spectrum of $\text{Cu}_3(\text{BTC})_2$ MOF.

International Journal for Research in Applied Science & Engineering Technology (IJRASET)

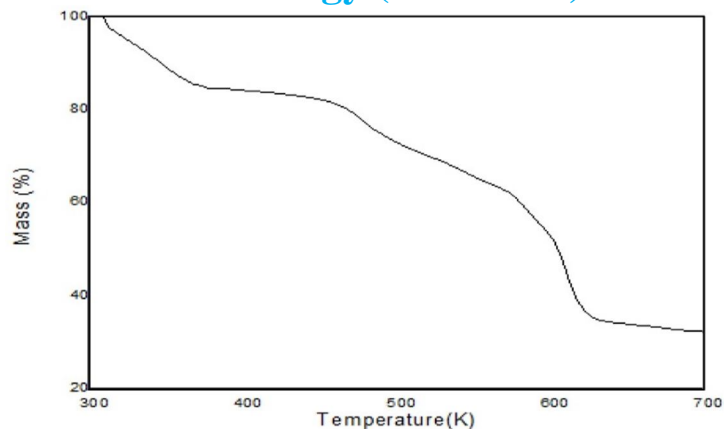


Fig. 4 TGA curve of Cu₃(BTC)₂ MOF.

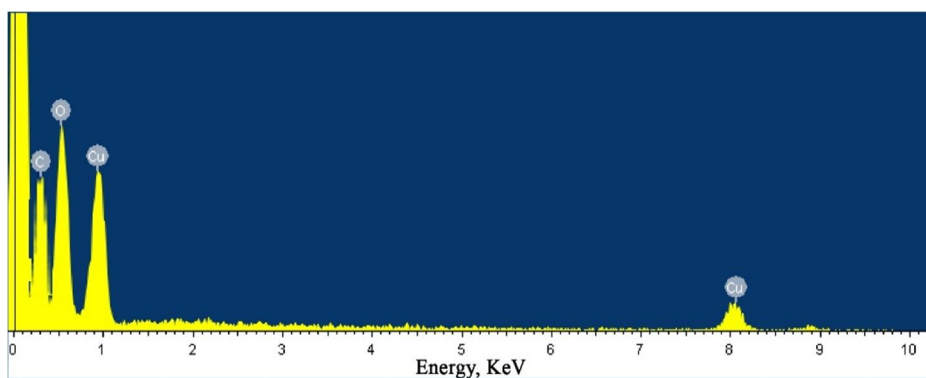


Fig. 5 EDXS pattern of Cu₃(BTC)₂ MOF.

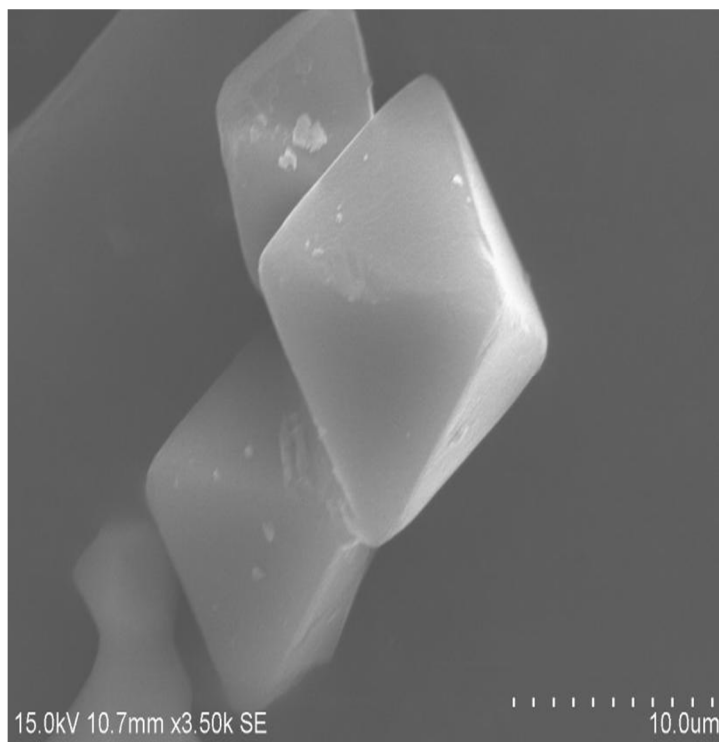


Fig. 6(a) SEM image of Cu₃(BTC)₂ MOF at 10 μ m.

International Journal for Research in Applied Science & Engineering Technology (IJRASET)

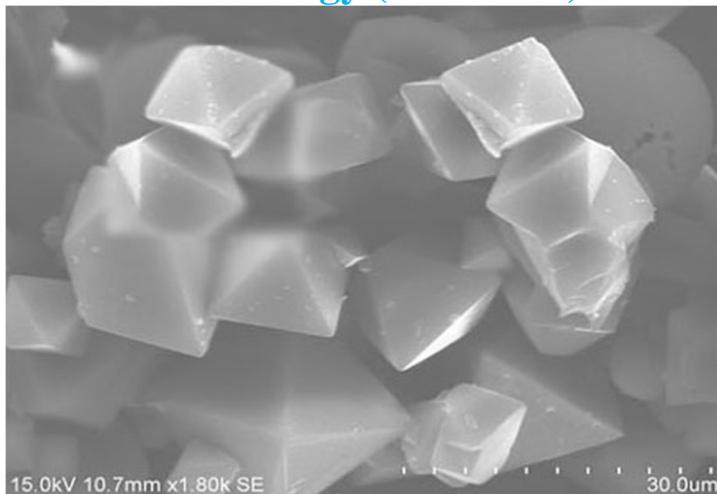


Fig. 6(b) SEM image of Cu₃(BTC)₂ MOF at 30 μm.

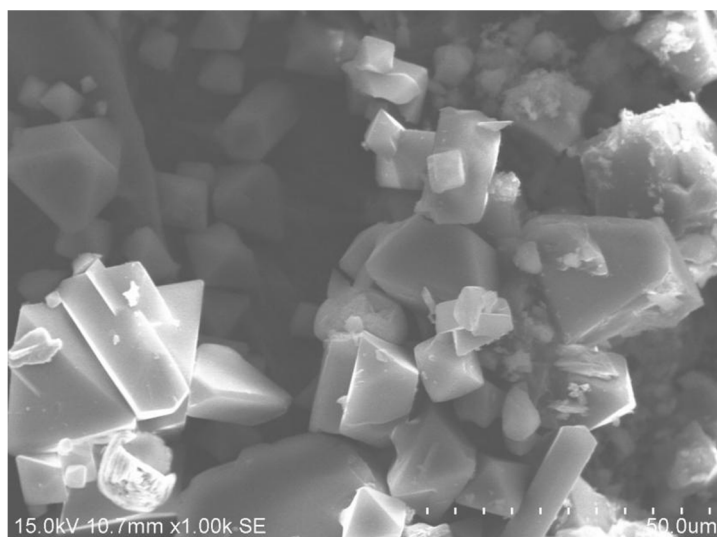


Fig. 6(c) SEM image of Cu₃(BTC)₂ MOF at 50 μm.

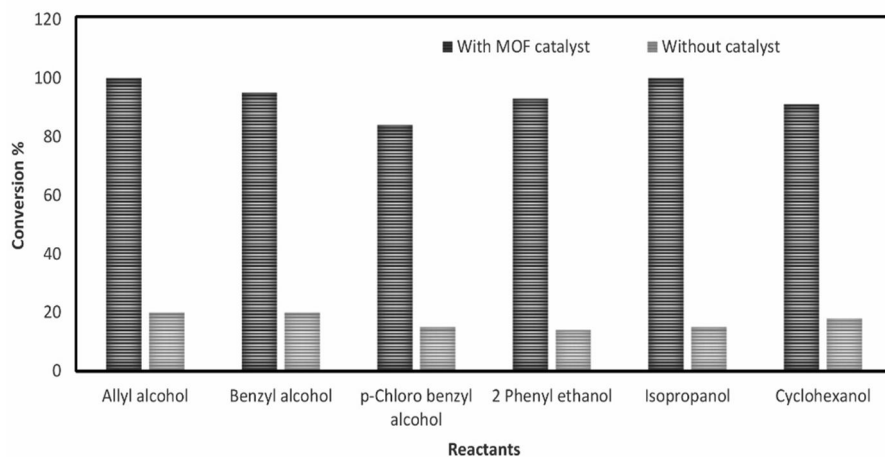


Fig. 7 Effect of catalyst on o-acetylation of alcohols over 20 wt% of MOF catalyst at 353 K.

International Journal for Research in Applied Science & Engineering Technology (IJRASET)

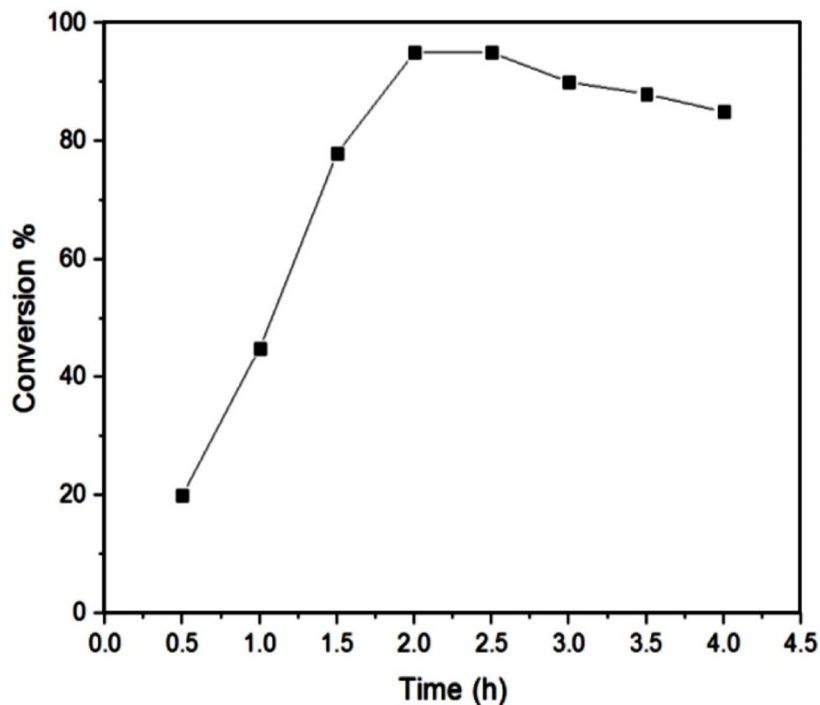


Fig. 8 Effect of time on o-acetylation of benzyl alcohols at 353 K.

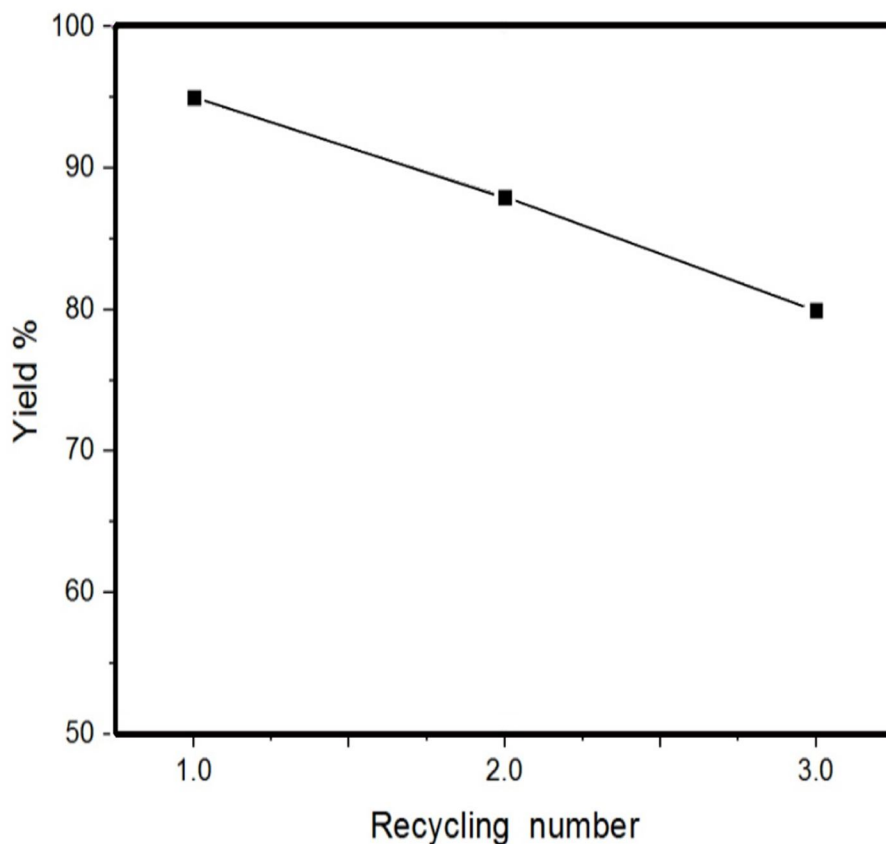


Fig. 9 Reusability of catalyst on o-acetylation of benzyl alcohol at 353 K.

International Journal for Research in Applied Science & Engineering Technology (IJRASET)

Table 1

Crystallographic data of $\text{Cu}_3(\text{BTC})_2$ MOF.

Empirical Formula	$\text{Cu}_3 \text{C}_{18} \text{O}_{12} \text{H}_6$
Formula weight	604.87
Crystal system	Tetragonal
Space group	p 4/mmm
a [Å]	7.31
b [Å]	7.31
c [Å]	6.96
α [°]	90°
β [°]	90°
γ [°]	90°
Volume [Å ³]	375
d [Å]	7.26
D crystallite size nm	48.15
Lattice strain	0.0071
Hkl	100

Table 2

Textural properties of $\text{Cu}_3(\text{BTC})_2$.

MOF	A_{BET} (m ² /g)	d_p (nm)	V_p (cm ³ /g)
$\text{Cu}_3(\text{BTC})_2$ *	257	6.64	0.173
$\text{Cu}_3(\text{BTC})_2$ **	700	8.01	0.431

* $\text{Cu}_3(\text{BTC})_2$ MOF before solvent exchange

** $\text{Cu}_3(\text{BTC})_2$ MOF after solvent exchange.

Table 3

EDXS data of $\text{Cu}_3(\text{BTC})_2$.

Element	Mass %	Atomic %
C K	35.86	51.48
O K	32.25	37.40
Cu K	31.89	11.12
TOTAL	100.00	100.00

International Journal for Research in Applied Science & Engineering Technology (IJRASET)

Table 4
Effect of temperature on O-acetylation of alcohols catalysed by Cu-BTC^a.

Entry	Reactant	Temperature (K)	Conversion (%)	Yield ^b (%)	Others (%)
1	Allyl alcohol	323	90	40 ^c , 50 ^d	10
		353	100	25 ^c , 75 ^d	-
		373	96	35 ^c , 61	4
2	Benzyl alcohol	323	87	87	13
		353	95	95	5
		373	89	89	11
3	p- Chloro benzyl alcohol	323	74	74	26
		353	84	84	16
		373	79	79	21
4	2- Phenyl ethanol	323	80	80	20
		353	93	93	7
		373	86	86	14
5	Isopropanol	323	92	32 ^c , 60 ^d	8
		353	100	31 ^c , 69 ^d	-
		373	96	35 ^c , 61 ^d	4
6	Cyclohexanol	323	80	80	20
		353	91	91	9
		373	83	83	17

^a Reaction conditions: alcohol = 2mmol; acetyl chloride = 4mmol; catalyst 20wt% (w.r.t.alcohol); time 2h under neat condition.

^b GC Yield.

^cProduct I and ^d Product II.

International Journal for Research in Applied Science & Engineering Technology (IJRASET)

Table 5

O-acetylation of alcohols catalysed by Cu-BTC^a.

Entry	Reactant	Conversion (%)	Product I	Product II	Yield ^{b,c} (%)		Others (%)
					PI	P II	
1		100			25.0	75.0	-
2		95		-	94.7	-	5.3
3		85		-	83.9	-	16.1
4		93		-	93.0	-	7.0
5		100			31.0	69.0	-
6		91		-	91.0	-	9.0

^aReaction conditions: alcohol = 2mmol; acetyl chloride = 4mmol; catalyst 20wt% (w.r.t. alcohol); time 2h under neat condition. ^bGC Yield. ^cTemperature 253 K

International Journal for Research in Applied Science & Engineering Technology (IJRASET)

Table 6

Effect of feed ratio on O-acetylation of benzyl alcohols at 353 K.

Feed ratio (alcohol : acetyl chloride)	Conversion (%)	Yield (%)	Others (%)
1:02	95	94.7	5.3
1:04	40	31.1	68.9
1:06	10	3.5	6.5

Catalyst 20 wt% of benzyl alcohol; temperature 353 K; time 2 h.



10.22214/IJRASET



45.98



IMPACT FACTOR:
7.129



IMPACT FACTOR:
7.429



INTERNATIONAL JOURNAL FOR RESEARCH

IN APPLIED SCIENCE & ENGINEERING TECHNOLOGY

Call : 08813907089  (24*7 Support on Whatsapp)